phys. stat. sol. (c) **1**, No. 11, 2650–2653 (2004) / **DOI** 10.1002/pssc.200405373

Interface and confined polar optical phonons in spherical ZnO quantum dots with wurtzite crystal structure

Vladimir A. Fonoberov and **Alexander A. Balandin** *

Nano-Device Laboratory, Department of Electrical Engineering, University of California–Riverside, Riverside, California 92521, USA

Received 15 May 2004, revised 13 August 2004, accepted 6 September 2004
Published online 17 November 2004

PACS 63.22.+m, 78.30.Fs, 78.67.Hc

We derive analytically the interface and confined polar optical-phonon modes for spherical quantum dots with wurtzite crystal structure. While the frequency of confined optical phonons in zincblende nanocrystals is equal to that of the bulk crystal phonons, the confined polar optical phonons in wurtzite nanocrystals are shown to have a discrete spectrum of frequencies different from those in bulk crystal. The calculated frequencies of confined polar optical phonons in wurtzite ZnO quantum dots are found to be in excellent agreement with experimental resonant Raman scattering data. The derived analytical expression for phonon modes can facilitate interpretation of experimental data obtained for ZnO quantum dots.

Several decades ago Englman and Ruppin [1] found that in quantum dots with zincblende crystal structure there exist confined phonon modes with the frequencies equal to those of bulk transverse optical (TO) and longitudinal optical (LO) phonons. It was also established that the interface phonon modes in such nanocrystals have frequencies intermediate between those of LO and TO modes. Recently, quantum dots with wurtzite crystal structure, such as GaN and ZnO nanocrystals, have attracted attention as promising candidates for optoelectronic and biomedical applications. Due to the uniaxial anisotropy, the phonon modes in wurtzite nanocrystals can differ substantially from those in zincblende nanocrystals. However, this issue has not been examined in detail and there exist only few reports [2, 3] on the approximate calculation of interface polar optical phonons in wurtzite GaN/AlN quantum dots. In this paper we show that unlike in zincblende nanocrystals, the spectrum of confined polar optical phonons in wurtzite nanocrystals consists of a series of discrete frequencies different from those of bulk LO and TO phonons.

Let us consider a spherical nanocrystal with the uniaxial anisotropy of the crystal lattice. The z-axis of the coordinate system is chosen to coincide with the symmetry axis of the nanocrystal. Within the framework of the dielectric-continuum approximation and Loudon's models for uniaxial crystals, the dielectric tensor for the nanocrystal can be written as

$$\hat{\varepsilon}(\omega)=\begin{pmatrix}\varepsilon_{\perp}(\omega) & 0 & 0\\ 0 & \varepsilon_{\perp}(\omega) & 0\\ 0 & 0 & \varepsilon_{z}(\omega)\end{pmatrix};\quad \varepsilon_{\perp(z)}(\omega)=\varepsilon_{\perp(z)}(\infty)\frac{\omega^{2}-\left(\omega_{\perp(z),\mathrm{LO}}\right)^{2}}{\omega^{2}-\left(\omega_{\perp(z),\mathrm{TO}}\right)^{2}}, \tag{1}$$

where $\varepsilon_{\perp}(\infty)$ and $\varepsilon_{z}(\infty)$ are optical dielectric constants, $\omega_{\perp,\mathrm{LO}}$ and $\omega_{z,\mathrm{LO}}$ are LO phonon frequencies, and $\omega_{\perp,\mathrm{TO}}$ and $\omega_{z,\mathrm{TO}}$ are TO phonon frequencies in bulk material. The exterior medium is considered to

* Corresponding author: e-mail: alexb@ee.ucr.edu, Phone: +1 909 787 2351, Fax: +1 909 787 2425

be optically inactive, e.g., air, plastic, glass, etc. In this case the dielectric tensor of the exterior medium reduces to a constant ε_D.

For polar optical phonons, the phonon potential $V_1(\mathbf{r})$ inside the nanocrystal and the phonon potential $V_2(\mathbf{r})$ outside the nanocrystal satisfy the Maxwell's equation:

$$-\nabla\left(\hat{\varepsilon}(\omega)\nabla V_1(\mathbf{r})\right)=0;\quad -\nabla\left(\varepsilon_D\nabla V_2(\mathbf{r})\right)=0 \tag{2}$$

with the boundary conditions

$$V_1(\mathbf{A})=V_2(\mathbf{A});\quad D_1(\mathbf{A})=D_2(\mathbf{A}), \tag{3}$$

where $\mathbf{A}\in S$ is the radius-vector of the surface *S* of the nanocrystal and

$$D_1(\mathbf{A})=\mathbf{n}_\mathbf{A}\left(\hat{\varepsilon}(\omega)\nabla V_1(\mathbf{r})\right)\Big|_{\mathbf{r}=\mathbf{A}};\quad D_2(\mathbf{A})=\mathbf{n}_\mathbf{A}\left(\varepsilon_D\nabla V_2(\mathbf{r})\right)\Big|_{\mathbf{r}=\mathbf{A}} \tag{4}$$

are the projections of the displacement vector **D** on the outer normal $\mathbf{n}_\mathbf{A}$ at the point **A**.

The inner part of the phonon potential $V_1(\mathbf{r})$ that satisfies Eq. (2) and is finite everywhere inside the nanocrystal and the outer part of the phonon potential $V_2(\mathbf{r})$ that satisfies Eq. (2) and vanishes far away from the nanocrystal can be found analytically in the prolate spheroidal coordinates (ξ, η, ϕ) and in the spherical coordinates (r, θ, ϕ), correspondingly:

$$V_1(\mathbf{r})=\frac{P_l^m(\xi)}{P_l^m\left(1/\sqrt{1-g(\omega)}\right)}P_l^m(\eta)\,e^{im\phi};\quad V_2(\mathbf{r})=\frac{a^{l+1}}{r^{l+1}}P_l^m(\cos\theta)\,e^{im\phi}, \tag{5}$$

where $g(\omega)=\varepsilon_z(\omega)/\varepsilon_\perp(\omega)$, a is the radius of the nanocrystal, P_l^m are associated Legendre polynomials of the first kind, and integers l ($l\ge 0$) and m ($|m|\le l$) are the quantum numbers of the phonon mode. The coordinates (ξ, η) and the coordinates (r, θ) are related as

$$\begin{cases} r\sin\theta=a\sqrt{1/g(\omega)-1}\,\sqrt{\xi^2-1}\,\sqrt{1-\eta^2}, \\ \sqrt{1/g(\omega)}\,r\cos\theta=a\sqrt{1/g(\omega)-1}\,\xi\,\eta. \end{cases} \tag{6}$$

In spherical coordinates the surface of the nanocrystal is defined as $r = a$. Substituting r for a in Eq. (6) we find that in the prolate spheroidal coordinates the surface of the nanocrystal is defined as $\xi=1/\sqrt{1-g(\omega)}$ together with $\eta=\cos\theta$. Thus, it is seen form Eq. (5) that the first boundary condition in Eq. (3) is satisfied. To find the normal components of the displacement vector **D** at the surface of the nanocrystal, we substitute Eq. (5) into Eq. (4). Using relation (6), it can be shown that the second boundary condition in Eq. (3) is satisfied only when the following equality holds:

$$\frac{\varepsilon_z(\omega)}{\sqrt{1-g(\omega)}}\frac{\partial\ln P_l^m(\xi)}{\partial\xi}\bigg|_{\xi=1/\sqrt{1-g(\omega)}}=-(l+1)\varepsilon_D. \tag{7}$$

Eq. (7) defines the spectrum of both interface and confined polar optical phonons in a spherical quantum dot with wurtzite crystal structure. Using the explicit form of the associated Legendre polynomials P_l^m, one can represent Eq. (7) in the following convenient form:

$$\sum_{n=0}^{\left\lfloor\frac{l-|m|}{2}\right\rfloor}\binom{l-|m|}{2n}\frac{(2n-1)!!(2l-2n-1)!!}{(2l-1)!!}\left(\frac{\varepsilon_\perp(\omega)}{\varepsilon_D}|m|+\frac{\varepsilon_z(\omega)}{\varepsilon_D}(l-|m|-2n)+l+1\right)\left(\frac{\varepsilon_z(\omega)}{\varepsilon_\perp(\omega)}-1\right)^n=0. \tag{8}$$

As seen from Eq. (8), there are no phonons with $l = 0$ and all phonon frequencies with $m \neq 0$ are twice degenerate with respect to the sign of m. It should be pointed out, that in the case of the isotropic spherical nanocrystal [$\varepsilon_{\perp}(\omega) = \varepsilon_{z}(\omega)$], Eq. (8) reduces to the equation $\varepsilon(\omega)/\varepsilon_{D} = -1 - 1/l$ found in Ref. [1] for interface optical phonons. Analyzing Eq. (8), one can find that for each pair (l, m) there is one interface optical phonon and $l - |m|$ confined optical phonons for $m \neq 0$ ($l - 1$ for $m = 0$).

Recently measured Raman scattering spectra of spherical wurtzite ZnO nanocrystals [4] have revealed confined polar optical phonons that have frequencies different from those of bulk LO and TO phonons and lying in the intervals ($\omega_{z,\mathrm{LO}}$, $\omega_{\perp,\mathrm{LO}}$) and ($\omega_{z,\mathrm{TO}}$, $\omega_{\perp,\mathrm{TO}}$). No quantitative explanation of the observed frequencies of the confined phonons has been given so far.

All frequencies of polar optical phonons with $l = 2$, 4 and $m = 0$, calculated as roots of Eq. (8), are listed in Table 1 (columns two and three). According to the experiment, we consider air with the dielectric constant $\varepsilon_{D} = 1$ as the exterior medium. Both optical dielectric constants $\varepsilon_{\perp}(\infty)$ and $\varepsilon_{z}(\infty)$ of wurtzite ZnO are taken equal to 3.7 [5]. Bulk LO and TO phonon frequencies of wurtzite ZnO are listed in the first column of Table 1. The calculated spectrum of phonons in wurtzite ZnO quantum dots can be divided into three regions: confined TO phonons ($\omega_{z,\mathrm{TO}} < \omega_{\mathrm{TO}} < \omega_{\perp,\mathrm{TO}}$), interface phonons ($\omega_{\perp,\mathrm{TO}} < \omega_{\mathrm{IO}} < \omega_{z,\mathrm{LO}}$), and confined LO phonons ($\omega_{z,\mathrm{LO}} < \omega_{\mathrm{LO}} < \omega_{\perp,\mathrm{LO}}$). The above division of the phonon modes into confined and interface phonons is based on the sign of the function $g(\omega)$ (interface phonons if $g(\omega) > 0$ and confined phonons if $g(\omega) < 0$). It is important to note that the frequencies of the interface optical phonons decrease substantially when ε_{D} increases, while the frequencies of the confined optical phonons decrease only slightly with increasing ε_{D} .

Table 1 Frequencies of polar optical phonons in ZnO quantum dots.

Bulk ZnO [1]	ZnO QD (calc.) [2] $l = 2$, $m = 0$	ZnO QD (calc.) [2] $l = 4$, $m = 0$	ZnO QD (exp.) [3] $R = 8.5$ nm	ZnO QD (exp.) [3] $R = 4.0$ nm
$\omega_{z,\mathrm{TO}} = 380$ cm^{-1}		$\omega_{\mathrm{TO}} = 393.7$ cm^{-1}	$\omega_{\mathrm{TO}} = 393$ cm^{-1}	$\omega_{\mathrm{TO}} = 393$ cm^{-1}
$\omega_{\perp,\mathrm{TO}} = 413$ cm^{-1}	$\omega_{\mathrm{IO}} = 534.0$ cm^{-1}	$\omega_{\mathrm{IO}} = 542.1$ cm^{-1}		
$\omega_{z,\mathrm{LO}} = 579$ cm^{-1}	$\omega_{\mathrm{LO}} = 587.8$ cm^{-1}	$\omega_{\mathrm{LO}} = 582.8$ cm^{-1}	$\omega_{\mathrm{LO}} = 588$ cm^{-1}	$\omega_{\mathrm{LO}} = 584$ cm^{-1}
$\omega_{\perp,\mathrm{LO}} = 591$ cm^{-1}		$\omega_{\mathrm{LO}} = 589.9$ cm^{-1}		

[1] Bulk values shown for comparison are after Ref. [5].
[2] Calculated values are the roots of Eq. (8).
[3] Experimental values are after Ref. [4].

Ref. [4] reports results of Raman spectroscopy of two samples with spherical wurtzite ZnO quantum dots carried out at room temperature. The two samples contained the powder of ZnO nanocrystals with diameters 8.5 nm and 4.0 nm, correspondingly. Since the excitation wavelength 363.8 nm (~ 3.41 eV) was very close to the exciton ground state energy for the 8.5 nm quantum dots [6], the spectrum of the first sample is the resonant Raman spectrum. Both spectra exhibited two peaks in the region of polar optical phonons: 393 cm^{-1} and 588 cm^{-1} for the first sample and 393 cm^{-1} and 584 cm^{-1} for the second sample (these frequencies are also shown in Table 1). As seen from Eq. (8), the spectrum of polar optical phonons in spherical nanocrystals does not depend on the size of the nanocrystal. However, a phonon line in the non-resonant Raman spectrum can be shifted due to the contribution from the excited exciton states. Moreover, smaller quantum dots may have stronger deviation from the spherical shape. Therefore, from our calculations we should expect that the frequencies 393 cm^{-1} and 588 cm^{-1} of the resonant Raman spectrum correspond to some of the discrete eigenfrequencies found from Eq. (8). Indeed, we can see it from Table 1 that the above two frequencies are the one of confined TO phonon with $l = 4$, $m = 0$ and the one of confined LO phonon with $l = 2$, $m = 0$.

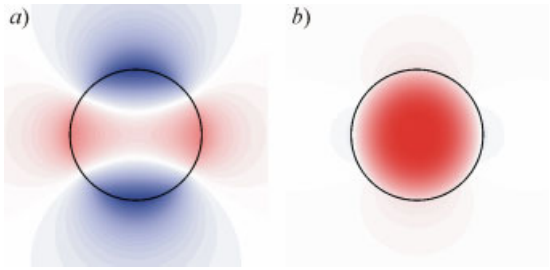

Fig. 1 Cross-sections of the phonon potentials for polar optical phonon modes with $l = 2$ and $m = 0$ in a ZnO quantum dot. The cross-sections are along the z-axis, which is directed vertically. Black circles indicate the boundary of the quantum dot. In the colour version, blue and red colours denote positive and negative values of the phonon potential, correspondingly. The frequencies of the depicted phonon modes (a) and (b) are given in the second column of Table 1 from top to bottom, respectively.

The dominant component of the wave function of the exciton ground state in spherical ZnO quantum dots is symmetric with respect to the rotations around z-axis or the reflection in the xy-plane [6]. Therefore, the selection rules for the optical phonon modes observed in the resonant Raman spectra of ZnO nanocrystals are $m = 0$ and $l = 2, 4, 6, \ldots$ The phonon modes with higher symmetry (smaller quantum number l) are more likely to be observed in the Raman spectra. In Fig. 1, the phonon potentials of all two phonon modes with $l = 2$ ($m = 0$) are shown. There is one interface phonon mode [Fig. 1(a)] and one confined LO phonon mode [Fig. 1(b)] in this case. In Fig. 2, the phonon potentials of all four phonon modes with $l = 4$ ($m = 0$) are shown. There is one confined TO phonon mode [Fig. 2(a)], one interface phonon mode [Fig. 2(b)], and two confined LO phonon modes [Figs. 2(c) and 2(d)] in this case. It is seen from Figs. 1 and 2, that the confined LO phonon mode with $l = 2$, $m = 0$ ($\omega = 587.8$ cm^{-1}) and the confined TO mode with $l = 4$, $m = 0$ ($\omega = 393.7$ cm^{-1}) are the confined modes with the highest symmetry among the confined LO and TO phonon modes, correspondingly. Therefore, they should give the main contribution to the resonant Raman spectrum. Indeed, they almost coincide with the experimentally recorded frequencies 588 cm^{-1} and 393 cm^{-1}.

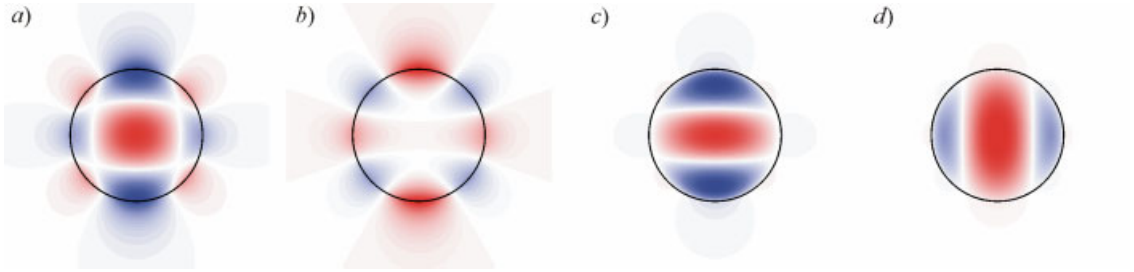

Fig. 2 Cross-sections of the phonon potentials for polar optical phonon modes with $l = 4$ and $m = 0$ in a ZnO quantum dot. The denotations are the same as in Fig. 1. The frequencies of the depicted phonon modes (a), (b), (c), and (d) are given in the third column of Table 1 from top to bottom, respectively.

Based on our analytical results we were able to explain quantitatively the positions of the polar optical phonon lines observed in the resonant Raman spectra of spherical wurtzite ZnO quantum dots. The obtained results allow one to accurately predict the frequencies of optical phonons in wurtzite nanocrystals.

Acknowledgements This work was supported in part by the NSF-NATO 2003 award to V. A. F. and CRDF award MP2-3044-CH-02 to A.A.B.

References

[1] R. Englman and R. Ruppin, Phys. Rev. Lett. **16**, 898 (1966); R. Englman, R. Ruppin, J. Phys. C **1**, 614 (1968).
[2] D. Romanov, V. Mitin, and M. Stroscio, Physica B **316/317**, 359 (2002).
[3] D. A. Romanov, V. V. Mitin, and M. A. Stroscio, Phys. Rev. B **66**, 115321 (2002).
[4] M. Rajalakshmi, A. K. Arora, B. S. Bendre, and S. Mahamuni, J. Appl. Phys. **87**, 2445 (2000).
[5] C. A. Arguello, D. L. Rousseau, and S. P. S. Porto, Phys. Rev. **181**, 1351 (1969).
[6] V. A. Fonoberov and A. A. Balandin, Phys. Rev. B, accepted for publication (2004).